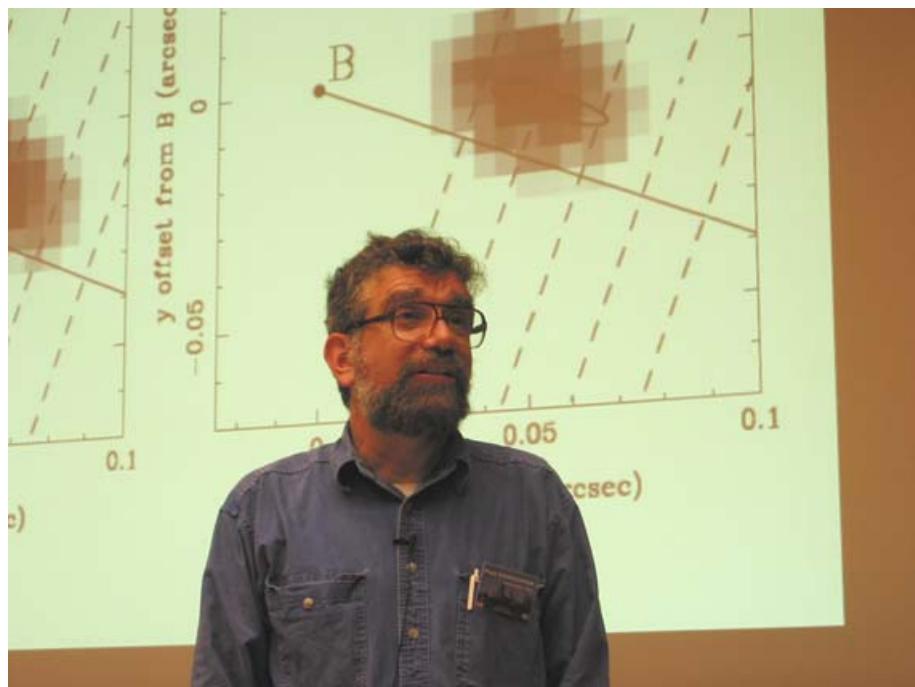# Part 4

Times Delays and Hubble Constant

Paul L. Schechter

Frédéric Courbin

The Hubble Constant from Gravitational Lens Time Delays

Paul L. Schechter[1]†

[1]Department of Physics, Massachusetts Institute of Technology, Cambridge, MA 02139, USA
email: schech@mit.edu

Abstract. Present day estimates of the Hubble constant based on Cepheids and on the cosmic microwave background radiation are uncertain by roughly 10% (on the conservative assumption that the universe may not be *perfectly* flat). Gravitational lens time delay measurements can produce estimates that are less uncertain, but only if a variety of major difficulties are overcome. These include a paucity of constraints on the lensing potential, the degeneracies associated with mass sheets and the central concentration of the lensing galaxy, multiple lenses, microlensing by stars, and the small variability amplitude typical of most quasars. To date only one lens meets all of these challenges. Several suffer only from the central concentration degeneracy, which may be lifted if one is willing to assume that systems with time delays are either like better constrained systems with non-variable sources, or alternatively, like nearby galaxies.

1. Context

Were we to choose at random a hundred members of the IAU and ask each of them to tell us the value of the Hubble constant and how it is measured, few if any would refer to gravitational lens time delay measurements. Most would instead refer to observations of Cepheid variables with HST or to observations of the CMB power spectrum with WMAP. These set the *de facto* standard against which time delay estimates must be evaluated.

The Cepheids give a Hubble constant of 72 km/s/Mpc with a 10% uncertainty (Freedman *et al.* 2001), a result that most of our randomly chosen astronomers would find relatively straightforward. But only a handful of them would be able to tell us how the CMB power spectrum yields a measurement of the Hubble constant.

In his opening talk, David Spergel told us that three numbers are determined to high accuracy by the CMB power spectrum: the height of the first peak, the contrast between the heights of the even and odd peaks, and the distance between peaks. Ask anyone who calls himself a cosmologist how many free parameters his world model has and the number N will be larger than three. Spergel's three numbers constrain combinations of those N parameters, but do not, in particular, tightly constrain the Hubble constant. One must supplement the CMB either with observations, or alternatively, with non-observational constraints.

The effects of supplementing the observed CMB power spectrum with other observations, and of adopting (or declining to adopt) non-observational constraints, are shown in table 1. All of the numbers shown are taken from the analysis by Tegmark *et al.* (2004b). They use the first year data from the Wilkinson Microwave Anisotropy Probe (Bennett et al. 2003), the second data release of the Sloan Digital Sky Survey (Abazajian *et al.* 2004), the Tonry *et al.* (2003), data for high redshift Type Ia supernovae, and data from 6 other CMB experiments: Boomerang, DASI, MAXIMA, VSA, CBI and ACBAR.

† Present address: Center for Space Research 37-664G, 77 Massachusetts Avenue, Cambridge, MA 02139, USA

Table 1. The CMB power spectrum and the Hubble constant

very-nearly flat			perfectly flat		
observations	Ω_{tot}	$100h$	observations	Ω_{tot}	$100h$
WMAP1	$1.086^{+0.057}_{-0.128}$	50^{+16}_{-13}	WMAP1	1	74^{+18}_{-7}
add SDSS2	$1.058^{+0.039}_{-0.041}$	55^{+9}_{-6}	add SDSS2	1	70^{+4}_{-3}
add SNae	$1.054^{+0.048}_{-0.041}$	60^{+9}_{-6}	add other CMB	1	69^{+3}_{-3}

We see from the first line of table 1 that the value of the Hubble constant derived from the WMAP1 data alone is a factor of 1.5 or 2.5 more uncertain than the Cepheid result, depending upon whether the universe is taken to be perfectly flat or only very-nearly flat. Combining the galaxy power spectrum as measured with SDSS2 (Tegmark *et al.* 2004a) reduces the uncertainties by factors of 3 and 2, respectively. In the very-nearly flat case, adding type Ia supernovae does little to change the uncertainty but shifts the value of H_0 closer to the Cepheid value. In the perfectly flat case, adding other CMB measurements reduces the uncertainty in H_0 by another factor of 1.3. Small deviations from flatness produce substantial changes in the Hubble constant, with the product $h\Omega_{tot}^5$ remaining roughly constant (Tegmark et al. 2004b).

Suppose we were to show table 1 to our randomly chosen IAU members and again ask them the value of the Hubble constant (and its uncertainty). Some would argue that the results for the very-nearly flat case are so very-nearly flat that it is reasonable to adopt perfect flatness as a working model. We observe that $|\log \Omega_{tot}| < 0.10$, when it might have been of order 100 (or perhaps 3 if one admits anthropic reasoning). But others would be reluctant to take perfect flatness for granted. The very sensitivity of the Hubble constant to that assumption would be an argument against adopting it. The present author is, himself, ambivalent.

2. H_0 from time delays *circa* 2003

Refsdal (1964) first proposed measuring the Hubble constant using gravitationally lensed supernovae 15 years before the discovery of the first gravitationally lensed quasar. In the past two years the status of Hubble constant measurements from time delays has been reviewed by Courbin (2003) and by Kochanek & Schechter (2004). Figure 1, taken from Courbin's review, summarizes his report. It should be noted that Courbin deliberately incorporated results representing diverse approaches to computing H_0. The average is one standard deviation smaller than the Cepheid result with a comparable uncertainty. It is also in agreement with the CMB results of table 1.

But if we were to make such a figure today, we might find it less reassuring. The H_0 value for PG1115+080 in figure 1 is based on a model for the lensing galaxy that is far from the fundamental plane for ellipticals. The value for RXJ0911+0554 is based on a faulty model (Schechter 2000) that the present author repudiates in §4.4. And the values for HE1104-1805 are based on a time delay that Ofek & Maoz (2003) have shown to be too large by a factor of two, driving the points off the top of the plot. The uncertainty in the Hubble constant, as derived from the scatter among systems, would be considerably larger today than it is in figure 1.

In what follows we discuss a number of major difficulties associated with using time delay measurements to measure H_0. All but one of the systems in figure 1 are subject
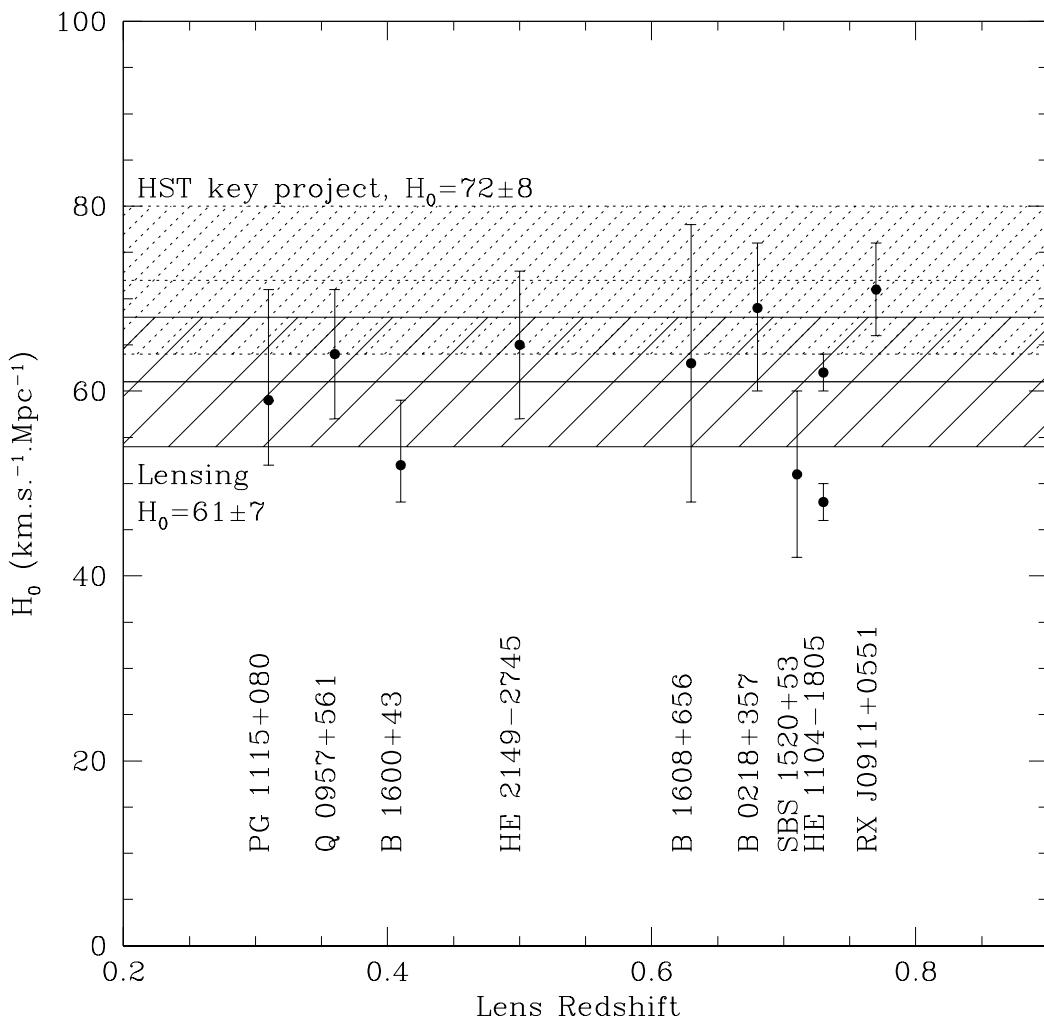
Figure 1. Time delay measurements of the Hubble constant, *circa* 2003 (Courbin 2003).

to one or more of these difficulties. Before delving into the details, we review the physics upon which the estimate of the Hubble constant is based.†

3. Lensing fundamentals

3.1. *The 3 D's*

There is a sense in which time delay is the most fundamental manifestation of gravitational lensing. In the weak field limit a gravitational potential produces an effective index of refraction that increases the travel time for a photon. Fermat's principle requires that the photon travel along a path that is a minimum, a maximum or a saddlepoint

† An excellent, although slightly outdated pedagogical treatment of gravitational lensing can be found in Narayan & Bartelmann (1999).

of the travel time. The photon must detour around the path it otherwise would have taken. A balance is struck between increased travel time associated with the detour (the geometric delay) and decreased travel time due to the shallower gravitational potential (the Shapiro delay),

$$\begin{pmatrix} \text{time} \\ \text{delay} \end{pmatrix} = \begin{pmatrix} \text{geometric} \\ \text{delay} \end{pmatrix} + \begin{pmatrix} \text{gravitational} \\ \text{delay} \end{pmatrix}. \tag{3.1}$$

If the size of the lens is small compared to the path length, we can use the thin lens approximation. The time delay can be expressed in terms of a two-dimensional effective potential obtained by integrating the gravitational potential Φ_{3D} along the line of sight,

$$\psi_{2D} = \frac{D_{LS}}{D_S} \int_{observer}^{source} \frac{2\Phi_{3D}}{c^2} \frac{d\ell}{D_L}. \tag{3.2}$$

It depends upon the angular diameter distances to the lens and to the source, D_L and D_S, and upon the distance from the lens to the source, D_{LS}. With this simplification all of gravitational lensing boils down to taking derivatives of the time delay function,

$$\tau = \frac{1+z_L}{H_0} \frac{d_L d_S}{d_{LS}} \left[\frac{1}{2}(\vec{\theta} - \vec{\beta})^2 - \psi_{2D}(\vec{\theta}) \right], \tag{3.3}$$

where $\vec{\theta}$ measures the position on the sky at which a ray crosses the plane of the lens and $\vec{\beta}$ is the position on the sky of the source. Here we use the dimensionless variants of the angular diameter distances, d_L, d_S, and d_{LS}. The quantity $\vec{\theta} - \vec{\beta}$ is the amount by which a ray is deflected. The geometric part of the time delay varies as the square of deflection in the limit of small deflections, a straightforward consequence of the Pythagorean theorem.

Differentiating τ with respect to $\vec{\theta}$ and setting the gradient of τ to zero allows us to solve for the minima, maxima and saddlepoints of the time delay. It gives what is often call *the* lens equation,

$$\vec{\theta} - \vec{\beta} - \vec{\nabla}\psi_{2D} = 0. \tag{3.4}$$

The deflection, $\vec{\theta} - \vec{\beta}$, is equal to the gradient of the two dimensional potential.

The magnification of an image is the ratio of the observed angular size to the true angular size of an object. We want something like the ratio of $\Delta\vec{\theta}$ to $\Delta\vec{\beta}$, but both of these are vectors. Passing to derivatives, the quantity $\partial\vec{\theta}/\partial\vec{\beta}$ gives a magnification matrix that maps a vector at the position of the source, $\Delta\vec{\beta}$, into a vector in the image plane, $\Delta\vec{\theta}$. This matrix cannot be calculated from equation 3.4 because the two dimensional potential is a function of position in the lens plane, not the source plane. But its inverse can be calculated by taking the derivative of equation 3.4 with respect to $\vec{\theta}$, giving the inverse magnification matrix,

$$\frac{\partial\vec{\beta}}{\partial\vec{\theta}} = \begin{pmatrix} 1 - \frac{\partial^2\psi}{\partial\theta_x^2} & -\frac{\partial^2\psi}{\partial\theta_x \partial\theta_y} \\ -\frac{\partial^2\psi}{\partial\theta_x \partial\theta_y} & 1 - \frac{\partial^2\psi}{\partial\theta_y^2} \end{pmatrix}. \tag{3.5}$$

This is readily inverted to give the magnification matrix, $\partial\vec{\theta}/\partial\vec{\beta}$. Since the magnification matrix is symmetric, there is a choice of coordinates for which it is diagonal. Those diagonal elements are in general unequal, stretching or compressing the image more in one direction than the other. The magnification matrix might equally well be called the distortion matrix.

It is often the case that the source and its images are very much smaller than the resolution of our observations. Gravitational lensing conserves surface brightness, but as the solid angle subtended by the image is usually different from that subtended by the

source, the observed flux is also different. The scalar magnification factor, μ, is given by

$$\mu = \left| \frac{\partial \vec{\theta}}{\partial \vec{\beta}} \right|. \tag{3.6}$$

The observable consequences of lensing are mnemonized with three "D's," each corresponding to a different derivative of the time delay function. The first derivative of the delay function gives a deflection. The second derivative gives a distortion. And the "zeroth" derivative is just the delay function itself.

3.2. *Modeling the lens*

The previous subsection illustrates the power of mathematics: an enormous amount of interesting astrophysics can be swept under the rug of a single function, the two dimensional gravitational potential, $\psi(\vec{\theta})$. If we knew ψ *a priori* we would long since have measured the Hubble constant. Instead we must construct models for our potentials, adjusting them to fit whatever observations can be brought to bear. Williams & Saha (2000) have developed a method for modeling lenses that avoids making detailed assumptions about the shape of the lensing potential (see also SAHA & WILLIAMS' contribution to the present proceedings), at the price of non-uniqueness. The present author takes the view that we know something about galaxy potentials and therefore would do well to start by assuming lensing galaxies are much like nearby galaxies.

A model which is both very simple and very useful is the singular isothermal sphere in the presence of an external tide,

$$\psi_{2D}(\vec{\theta}) = br + \frac{\gamma}{2}r^2 \cos 2(\phi - \phi_\gamma). \tag{3.7}$$

The leading (monopole) term is the projection of the isothermal's potential. In our case the strength of the isothermal is parameterized by b, the radius of its Einstein ring. The tidal term is a quadrupole, and is parameterized by a dimensionless strength, γ, and an orientation ϕ_γ. Note that here we represent angular position on the sky, $\vec{\theta}$, in terms of polar coordinates r and ϕ, with r measured in radians.

The singular isothermal sphere gives the flat rotation curves characteristic of nearby galaxies. A substantial fraction of quadruple gravitational lenses are the result of strong tides from a group or cluster of galaxies of which the lens is a member. In the absence of these tides the lenses would produce only double images. The intrinsic flattening of the lensing galaxy also produces a quadrupole term (which has a different radial dependence), but the tidal contribution is usually considerably larger.

Our simple model does great injustice to the complexity of individual lenses, but complexity is a luxury we cannot afford. A parameterized model can have at most as many parameters as the available observable quantities and we are quite limited. The numbers of observables are summarized in table 2. Delay is a scalar, deflection is a two dimensional vector and the symmetric distortion matrix has three independent elements. We have subtracted one deflection from our available constraints because we do not know the position of the source. Likewise we subtract one distortion because we do not know

Table 2. Constraints

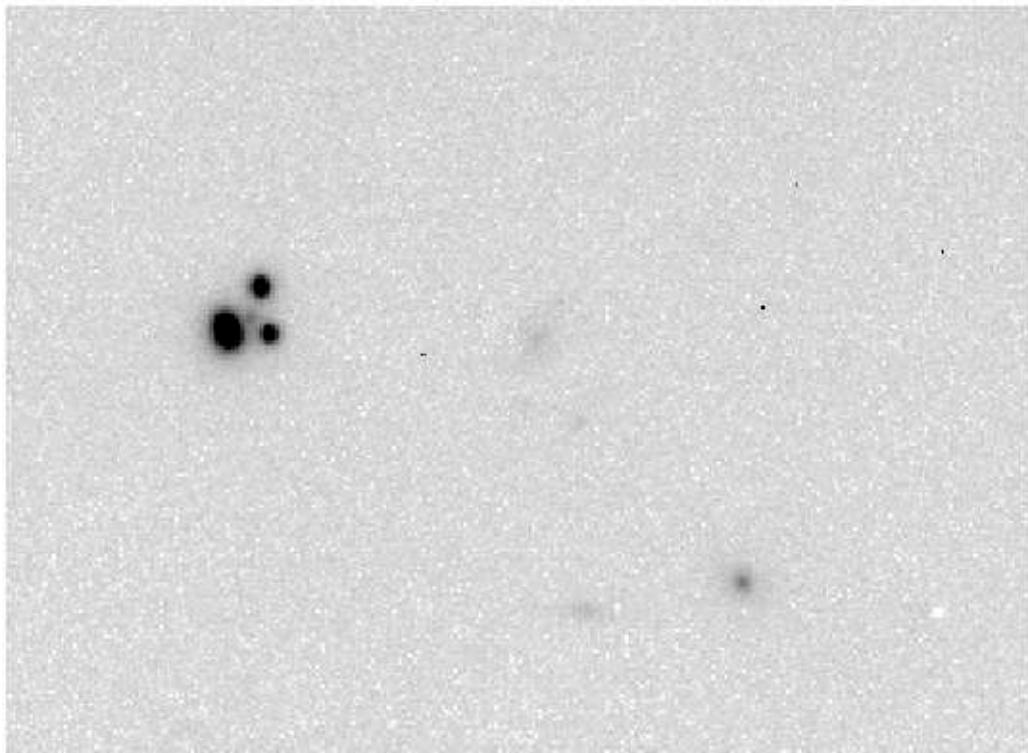|	
Delays:	$1 \times [\#images - 2]$
Deflections:	$2 \times [\#images - 1]$
Distortions:	$3 \times [\#images - 1]$
(or for unresolved sources)	
magnifications:	$1 \times [\#images - 1]$

Figure 2. The quadruple lens PG1115+080, observed with the Baade 6.5-m telescope. The small group of galaxies to the upper right lies very close to the position predicted from the positions of the four quasar images. It lies at the same redshift as the lensing galaxy.

the size and shape of our source (taking it to be elliptical). By the same argument we subtract one delay because we do not know the absolute time at which some event used to calculate delays actually occurred. In the case of delays we subtract a second delay because we need it to calculate the Hubble constant. It cannot be used *both* to constrain our model *and* to give H_0.

The situation is even worse if the images are not resolved by our telescopes. In such cases we measure only the fluxes of the images and get only one number from each distortion rather than three. Consider the case of a lensed quasar with two unresolved images. After discounting for the unknown properties of the source and reserving one delay for measuring H_0 we have only three constraints for our model. Using even our very simple model we are guaranteed a perfect fit, with no additional degrees of freedom left to check goodness of fit.

With no sanity check on our model, such doubles can be used only with extreme caution. Something might be amiss and we would have no way of knowing it. Moreover we cannot add additional parameters (allowing, for example, for the shape of the galaxy) because we have exhausted our supply of constraints. Four of the nine systems in figure 1 are just such doubles: B1600+43, HE2149-2745, SBS1520+53 and HE1104-1805.

The situation is slightly improved for four image systems. It is likewise slightly improved if there are multiple sources, as is sometimes the case for radio AGN. In constructing a list of major difficulties faced in measuring H_0, the first would be the paucity of constraints.

4. Problem lenses

4.1. *Kochanek's time delay formulation*

The system PG1115+080 illustrates another of the major difficulties in time delay measurements of H_0. The mathematics is simpler if we diagonalize the magnification matrix and introduce two dimensionless quantities, the convergence κ and the shear γ.

$$\frac{\partial \vec{\theta}}{\partial \vec{\beta}} = \begin{pmatrix} \frac{1}{1-\kappa-\gamma} & 0 \\ 0 & \frac{1}{1-\kappa+\gamma} \end{pmatrix}. \tag{4.1}$$

The convergence is the two-dimensional Laplacian of the two-dimensional potential,

$$\kappa = \frac{1}{2}\nabla_\theta^2 \psi, \tag{4.2}$$

and is therefore proportional to the surface mass density.

For zero shear, a convergence of unity gives infinite magnification in both directions. For zero convergence (which means zero surface density), a shear of unity gives infinite stretching in one direction. For a point mass there is unit shear everywhere on its Einstein ring.

KOCHANEK (2002; present proceedings) has shown that with these definitions we can write an expression for the difference in time delay between two images in a circularly symmetric system that depends to first order only upon the positions of the images with respect to the lens and the convergence averaged over the annulus bracketted by the two images.

$$\tau_B - \tau_A \simeq \left[\frac{1+z_l}{H_0}\right] \left[\frac{d_l d_s}{d_{ls}}\right] (|\vec{\theta}_A|^2 - |\vec{\theta}_B|^2) \times \left[1 - \langle\kappa\rangle + \mathcal{O}\left(\frac{|\vec{\theta}_B| - |\vec{\theta}_A|}{|\vec{\theta}_B| + |\vec{\theta}_A|}\right)^2\right]. \tag{4.3}$$

For power law density profiles, $\rho \sim r^{-\eta}$, we have

$$\langle\kappa\rangle \simeq \frac{3-\eta}{2}. \tag{4.4}$$

Notice that if $\eta = 2$, as would hold for an isothermal sphere, the average value of the convergence is one half. As $\eta \to 3$, approaching the central concentration for a point mass, $\langle\kappa\rangle \to 0$ and the predicted time delay is twice as long as in the isothermal case.

4.2. *The mass sheet degeneracy*

Kochanek's parameterization illuminates two different difficulties in measuring H_0 from time delays. Figure 2 shows PG1115+080 and its immediate surroundings. A fit of our simple model to the image positions indicates that the source of the tide lies along a line passing through the lensing galaxy and the upper right corner of the figure. At the cost of one additional parameter, we can substitute a second isothermal sphere for the tidal shear. This very much improves the fit, and the derived position is coincident with the small group of galaxies to the upper right of the lensed system. The inferred velocity dispersion for the second isothermal sphere is 375 km/s (Schechter *et al.* 1997), typical of a small group. The observation of a group at the position "predicted" by the simple model inspires confidence in it.

But if the group is isothermal, it has a convergence associated with it – in this case approximately 10%. This decreases the predicted time delay by 10%. Small numbers make measurement of the actual velocity dispersion difficult, but it is consistent (Tonry 1998) with the tidal estimate. Many of the quadruple lenses live in groups and clusters with

Table 3. Exponents for power law density profiles: $\rho \sim r^{-\eta}$

lensing galaxy	η	reference
JVAS0218+357	$1.96^{+0.02}_{-0.02}$	Wucknitz, Biggs, & Browne (2004)
Q0957+561	1.84	Barkana *et al.* (1999)
MG1131+0456	$2.40^{+0.2}_{-0.2}$	Chen, Kochanek, & Hewitt (1995)
PMN1632-0033	$1.91^{+0.02}_{-0.02}$	Winn, Rusin, & Kochanek (2004)
MG1654+1346	$1.90^{+0.16}_{-0.01}$	Kochanek (1995)
CLASS1933+503	$1.86^{+0.17}_{-0.11}$	Cohn, Kochanek, McLeod, & Keeton (2001)
$<\ \ >$	1.98	

convergences at the position of the lens of 10, 20 and even 30%. The corrections are substantial, and we must wonder whether we have got the cluster convergence correct. Two of the systems in figure 1, Q0957+561 and RXJ0911+0554, have inferred convergences in the 20 - 30% range. This is a manifestation of a difficulty more generally known as the mass sheet degeneracy (Gorenstein, Shapiro, & Falco 1988; Saha 2000). There is no way of knowing (from deflections and distortions) whether or not a mass sheet is present, but it affects the predicted time delays by changing the mean convergence.

4.3. *The central concentration degeneracy*

Equations 4.3 and 4.4 tell us that the interpretation of the time delay for PG1115+080 depends crucially upon the internal structure of the galaxy. An error in the radial exponent of plus or minus 0.1 produces a 10% change in the predicted time delay as compared to an isothermal model. Fortunately we can test the isothermality hypothesis. For an isothermal sphere, the angular radius of the Einstein ring, b, is directly proportional to the square of the velocity dispersion, σ^2:

$$b = \frac{d_{LS}}{d_S} 4\pi \frac{\sigma^2}{c^2} \tag{4.5}$$

With an Einstein ring radius $b = 1''15$, a lens redshift $z_L = 0.31$ and a source redshift $z_S = 1.71$ we predict $\sigma_{SIS} = 232$ km/s. This must be reduced by a factor $\sqrt{(1 - \kappa_{group})}$ which amounts to a 5% correction in the present case. We can test our prediction, but the measurement is a difficult one. The lensing galaxy is crowded by four very much brighter images. Tonry (1998) measures a velocity dispersion of 281 ± 25 km/s, very much larger than predicted. Treu & Koopmans (2002) use Tonry's measurement in modeling PG1115+080 and derive a value for H_0 very much larger than under the isothermal hypothesis. Their value is the one plotted in figure 1.

Why are we so reluctant to abandon the isothermal hypothesis for PG1115+080? First, because velocity dispersion estimates from equation 4.5 for an ensemble of lensing galaxies are consistent with the fundamental plane relation for non-lensing ellipticals. PG1115+080 is in no way unusual (Kochanek et al. 2000), but would be if we adopted the direct measurement.

A second argument is that the lenses for which we *can* measure the radial exponent are very nearly isothermal. Lenses with multiple sources, rings or central images all break the central concentration degeneracy and permit measurement of the radial exponent η. The results for six systems are shown in table 3 (see also WAYTH's contribution to the present proceedings). While there are differences in the way η was calculated for each of these systems, the results are consistent with isothermal. Unfortunately only one of these systems, JVAS0218+357, is also a system that has a measured time delay.
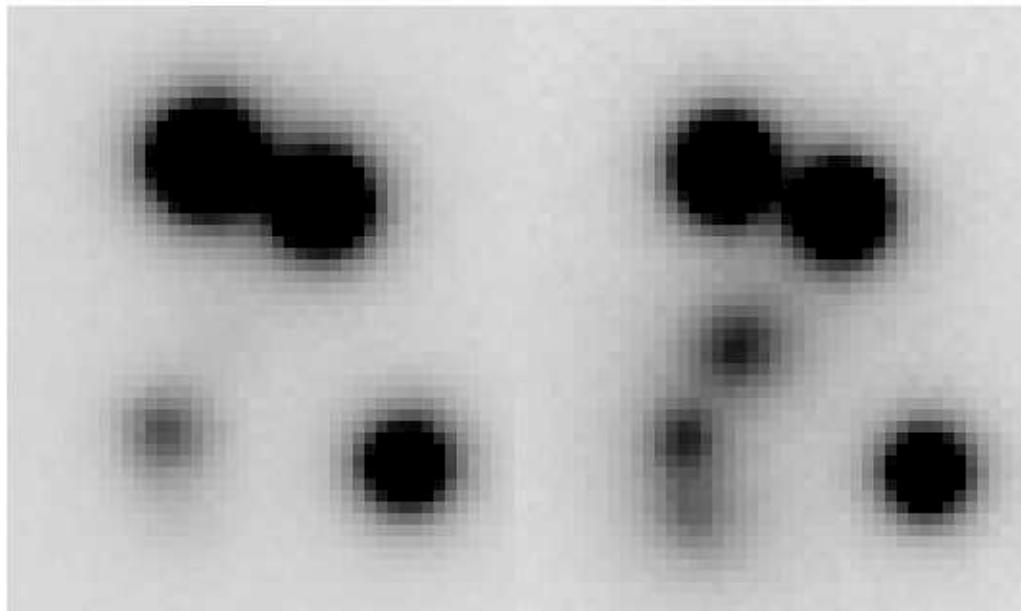
Figure 3. The quadruple system HE0230-2130, observed with the Baade 6.5-m telescope through g' (left) and i' (right) filters. The two red objects are lensing galaxies. The image between the two galaxies is a saddlepoint of the time delay function.

A third argument is that a great many nearby galaxies have been studied, and their potentials are consistent with isothermals. This is nicely shown in a figure published by Romanowsky & Kochanek (1999). For a sample of twenty bright ellipticals, the circular velocity inferred from the velocity dispersion declines only slightly over a factor of 30 in radius. The corresponding decline in PG1115+080, computed from its measured central dispersion and the Einstein ring radius, is very much larger. It is nonetheless true that the potentials for nearby ellipticals are only very-nearly isothermal and not perfectly isothermal. The central concentration degeneracy qualifies as another major difficulty associated with time delay estimates of H_0.

4.4. *Multiple lenses*

Another problem associated with modeling lensing galaxies is illustrated by the system HE0230-2130. There is not one lensing galaxy, but two, as seen in figure 3. The second, fainter galaxy provides the quadrupole moment that makes this a 4-image system and not a 2-image system. When we see two galaxies separated by only a few kpc, we must wonder how the non-baryonic matter is distributed. Are the halos for the two galaxies distinct? Or have they merged? How many components should we model? And where should their centers be? In such a case something with elements of the Williams & Saha (2000) form-free approach might be preferable to a straightforward parameterized model.

The system with the best time delays is CLASS1608+656. Fassnacht, Xanthopoulos, Koopmans, & Rusin (2002) have measured four beautiful radio lightcurves. All four time series faithfully reproduce the many bumps and wiggles. The multiple delays in this case are good enough to provide meaningful additional constraints to the deflections and distortions. But modeling the system is not straightforward. As with HE0230-2130, there are two lensing galaxies (figure 4) that appear to be interacting. A dust lane encircles
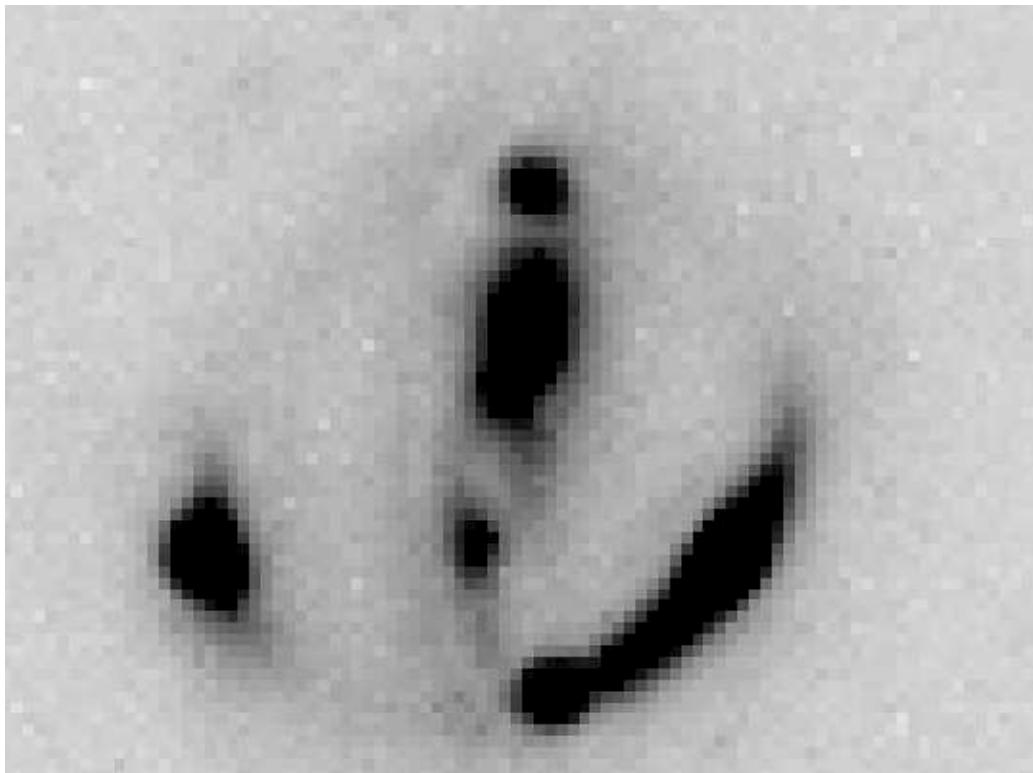
Figure 4. The quadruple system CLASS1608+656, observed with the Hubble Space Telescope through the $F814W$ filter. The lensing galaxies are marked $G1$ and $G2$. A dust lane can be seen encircling them.

them both. Again the question of how the dark matter might be distributed looms as crucial. Koopmans *et al.* (2003) have worked exceedingly hard to constrain this system, measuring positions for the images, the shape of the ring, and measuring the velocity dispersion of the more massive lens. We can nonetheless imagine a devil's advocate coming up with a plausible dark matter distribution uncorrelated with the observed galaxies that gives a very different value for the Hubble constant.

The problem of multiple lenses can be serious even when one of the galaxies is very much smaller than the principal lens. Consider the case of RXJ0911+0554, shown in figure 5, where the primary lensing galaxy has a faint companion. Given its faintness and our aversion to adding additional parameters, we might be tempted to ignore it, as did Schechter (2000) in the model used by Courbin to construct figure 1. But allowing for a mass at the position of this dwarf companion changes the predicted time delay by 10%. Though the smaller galaxy is a factor of 10 fainter than the primary lensing galaxy, its effect is to move the center of mass closer to the midpoint of the images, decreasing the differences in path length.

There is an irony here in that the multiple lenses work to our advantage in producing (or adding to) the quadrupole moments that give us 4 images rather than 2. But at the same time they make modeling considerably more difficult.
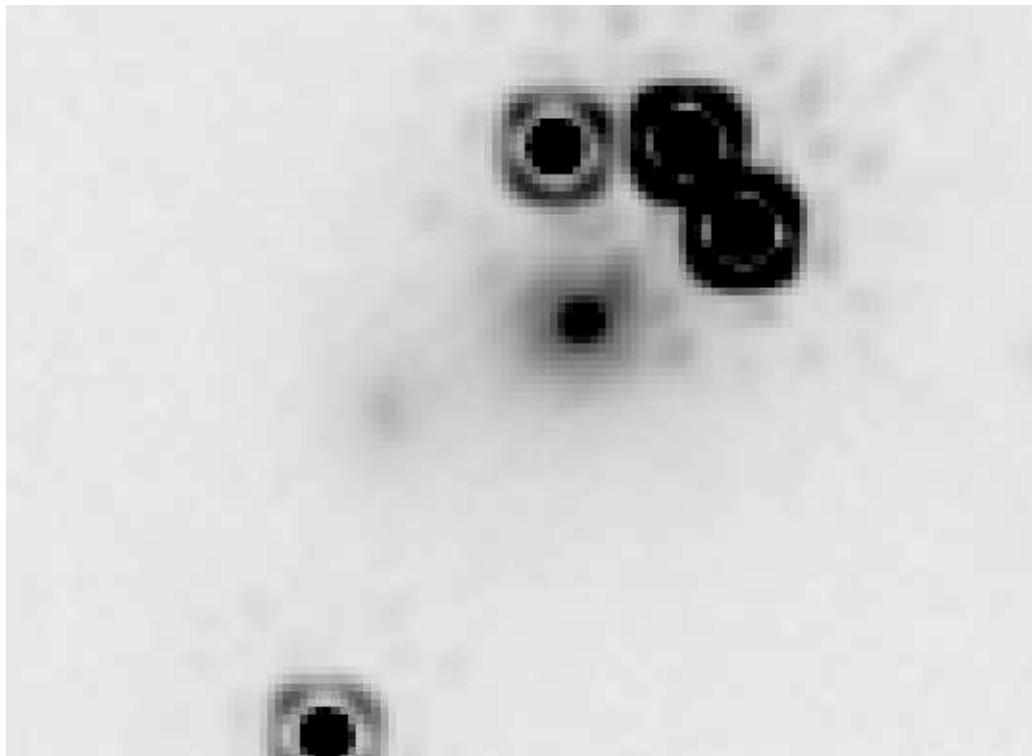
Figure 5. The quadruple system RXJ0911+0554, observed by the CASTLES consortium with the Hubble Space Telescope through the $F160W$ filter. The primary lensing galaxy $G1$ has a dwarf satellite $G2$. Allowing for the mass of the dwarf changes the derived value of H_0 by 10%.

4.5. *Microlensing*

In his contribution to the present proceedings, Lutz WISOTZKI presents spectroscopic evidence for microlensing of quasars. This has important consequences (unfortunately negative) for time delay estimates of H_0. It means that there are uncorrelated variations in the fluxes of images, especially in the optical continuum. The timescale for these fluctuations depends upon the size of the Einstein ring of the microlenses and upon the relative velocity of the quasar and the lensing galaxy. Taking the lenses to be a solar mass and the relevant velocities to be of order 300 km/s gives timescales of order 10 - 30 years. This ought not to matter for quasars lensed by galaxies, whose time delays are at most one year. But there have been repeated instances of uncorrelated variations in quasar lightcurves on considerably shorter timescales (e.g. Burud *et al.* 2000), in some cases causing considerable dispute about which points ought and ought not to be included in a time delay measurement and about the nature of the fluctuations.

Seven years ago the present author prevailed upon Andrzej Udalski to monitor HE1104-1805 for a time delay with the OGLE telescope (Udalski, Kubiak, & Szymański 1997). The OGLE group was at that time focussing exclusively on LMC and galactic bulge microlensing, but HE1104-1805 is at a very different right ascension. Three years of superb OGLE data were obtained in which no believable correlated variations were observed. But there were appreciable uncorrelated variations, most of which were attributable to
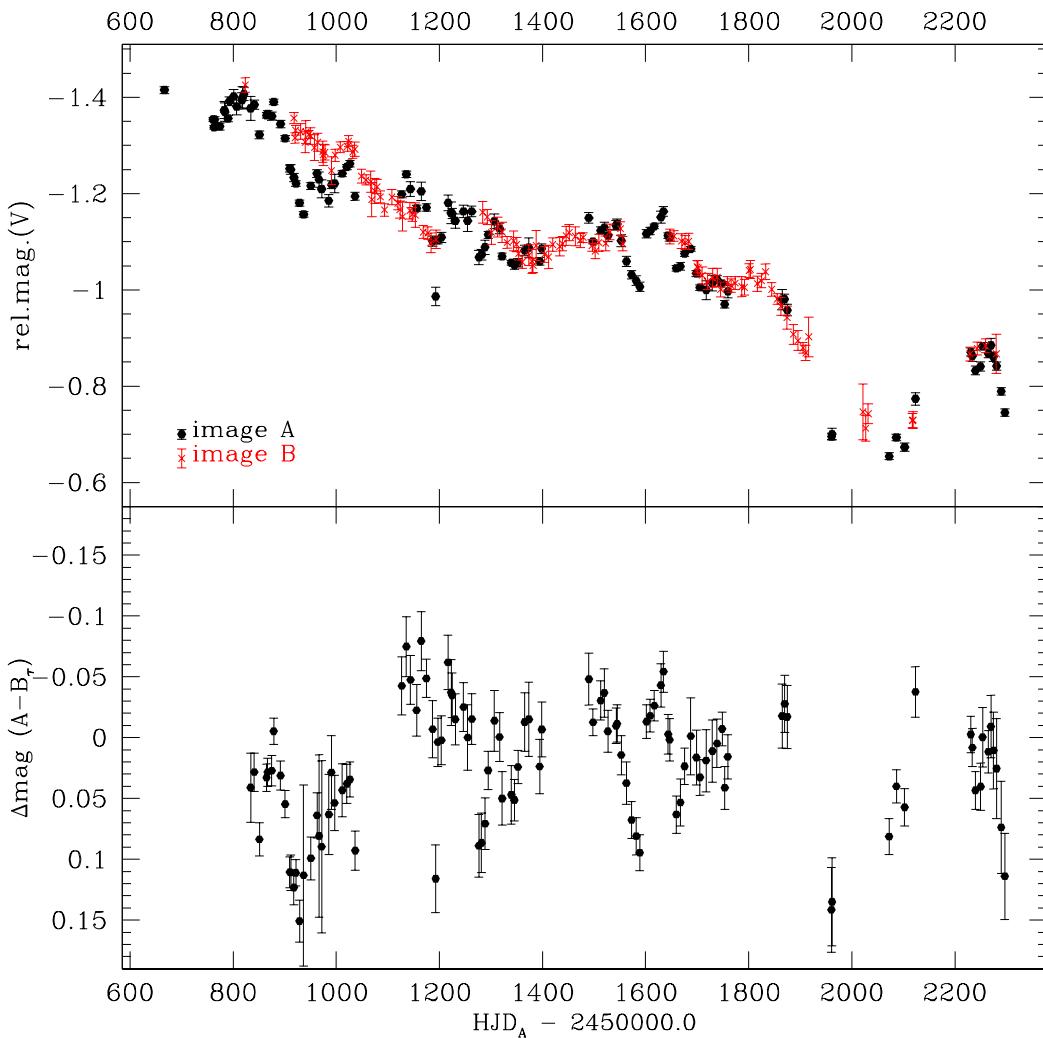
Figure 6. Lightcurves for the two components of HE1104-1805, taken with the OGLE 1.3-m telescope (Wyrzykowski et al. 2003). Note that while the measurement uncertainties are larger for the fainter, B image, the scatter is larger for the brighter, A image.

the brighter of the two images. After three years we admitted defeat and wrote a paper about microlensing (Schechter et al. 2003) which was, after all, OGLE's primary mission. The OGLE telescope was out of commission for upgrades during much of the following year; a few data points were obtained but were never reduced. But by then Ofek & Maoz (2003) had begun monitoring HE1104-1805 at the Wise Observatory. They used our data in conjunction with theirs to give a time delay that differed by a factor of two from the one used in figure 1. After Ofek and Maoz published their delay, Wyrzykowski *et al.* (2003) reduced the remaining OGLE data, confirming their value and giving the lightcurves in figure 6.

Notice that the error bars are smaller for the A image, yet the lightcurve is smoother for the B image. Image A appears to vary with an amplitude of 0.06 magnitudes on a

timescale of one week. The interpretation of these fluctuations is somewhat speculative, but there is no question that microlensing represents an another difficulty for time delay measurements of H_0.

4.6. *The myth of quasar variability*

One last difficulty associated with estimating H_0 is implicit in the fact that only 10% of the hundred or so known lensed quasars appear in figure 1. When we think of quasar variability we think of 3C273 or 3C279 and variations of a magnitude or more. But those quasars are well known precisely because of their variability. Most quasars are considerably more boring. Systematic studies of quasar variability at optical wavelengths consistently give rms fluctuations of order 10 - 15% on proper timescales of one year (Cristiani et al. 1996; Vanden Berk et al. 2004).

The good news is that a few quasars vary more than this. The bad news is that most vary even less than this. The statistics may be somewhat better for radio quasars, but then radio loud systems constitute only 10% of all quasars. While the small amplitude of quasar variations may give graduate students (mostly those working at radio wavelengths) an opportunity to show their skill in beating down their observational errors, flat lightcurves don't lead to offers of prestigious postdocs. It should be noted that there is considerable room for improvement in the optical lightcurves, for which the observational errors are much larger than photon statistics would imply. Our list of major difficulties in measuring H_0 has grown to include the following:

- the paucity of constraints,
- the mass sheet degeneracy,
- the central concentration degeneracy,
- multiple lenses,
- microlensing and
- small variability amplitudes.

5. A golden lens

The difficulties we have described are sufficiently common that almost every lensed quasar is subject to at least one of them. In general (though there are important exceptions) the double systems suffer from a paucity of constraints. Many quadruples suffer either from the mass sheet degeneracy (due to a nearby cluster) or from multiple lensing galaxies. Only a few systems (mostly radio loud quasars) have multiple sources permitting unambiguous determination of a radial density exponent. Are there *any* lenses which are not obviously subject to one or another of these difficulties?

A decade ago we imagined finding a "perfect" (Press 1996) or "golden" lens (Williams & Schechter 1997) that would permit determination of H_0 with small uncertainty. A lens that was not subject to any of the above difficulties might reasonably qualify for certification as a golden lens.

The system JVAS0218+357 (Patnaik et al. 1992) is such a system. It is a radio double that, at VLBI resolution, has a core and a blob (Biggs et al. 2003) of the sort that radio astronomers fancifully call jets. The double source breaks the concentration degeneracy, and implies an isothermal potential. Wucknitz, Biggs, & Browne (2004) have modeled the radio data, finding the radial exponent and the center of symmetry of the lensing potential (see also WUCKNITZ' contribution to the present proceedings). The time delay has been measured with better than 5% accuracy (Biggs *et al.* 1999).

But even this system is not 24 carat gold. The pairs of images are separated by only $0''\!.33$, implying a low luminosity lens, almost certainly not an elliptical. York *et al.* (2004)
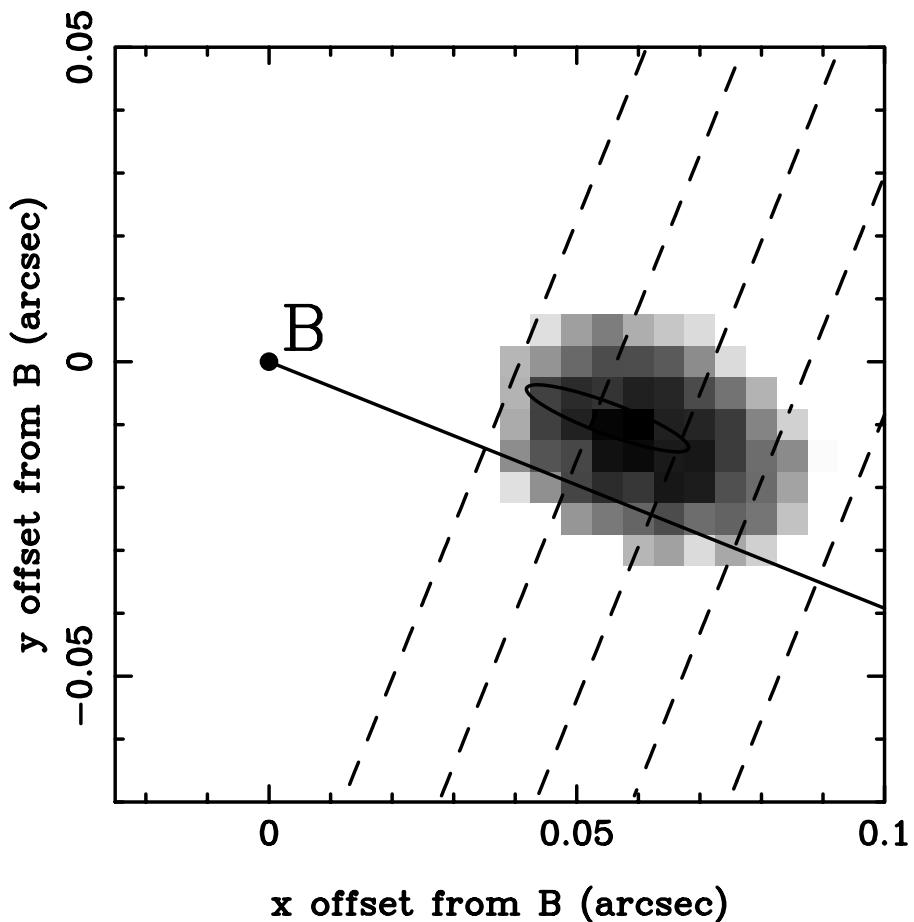
Figure 7. The shading of the pixels indicates relative likelihood for the optical position of the galaxy lensing JVAS0218+357 (York *et al.* 2004). The solid line is drawn from the *B* image toward the *A* image, which lies beyond the plot boundary. The diagonal dashes indicate loci of constant Hubble constant, starting with $H_0 = 90$ km/s/Mpc on the left and decreasing in steps of 10 km/s/Mpc. The elliptical contour gives the 2σ confidence region for the center of the lensing potential, as derived from radio observations of the lensed radio source by Wucknitz, Biggs, & Browne (2004).

have co-added data from a large number of HST orbits (see also JACKSON AND YORK'S contribution to the present proceedings). After careful PSF subtraction of the two quasar images, their data clearly shows an M101-like spiral. The residuals from PSF subtraction crowd the nucleus of the galaxy, making it difficult to measure its centroid accurately. The position of the center is crucial because of the strong dependence of the differential delay on the image distances. The agreement between the York *et al.* optical position and the Wucknitz center of symmetry is excellent (figure 7). The radio position gives $H_0 = 78 \pm 6$ km/s/Mpc (2σ uncertainty).

The work on JVAS0218+357 is remarkable for the range of astronomical techniques and resources that have been brought to bear on the system. It was discovered (Patnaik *et al.* 1992) and monitored (Biggs *et al.* 1999) at radio wavelengths using the VLA and Merlin. The global VLBI data (Biggs *et al.* 2003) are crucial to the modeling. The redshift for the lens (Browne, Patnaik, Walsh, & Wilkinson 1993) required large ground based

optical telescopes. Measuring the position of the lensing galaxy required HST (York *et al.* 2004), as is the case for most lenses.

6. Summary and Prospects

By the standards set forth in this paper, only one gravitationally lensed quasar qualifies as a golden lens. Taken by itself it gives a Hubble constant with a formal uncertainty as small or smaller than that obtained with Cepheids. But prudence demands at least one more golden lens before declaring that lenses do as well as (let alone better than) Cepheids.

The remaining systems with time delay measurements are not without value. The central concentration degeneracy may reasonably be lifted by appeal to other (non-variable) lensed systems for which the central concentration *can* be measured, or alternatively, by appeal to measurements of gravitational potentials of nearby elliptical galaxies. The present author would guess that the systematic errors associated with either of these assumptions would introduce an error of perhaps 5% in the Hubble constant. This would rehabilitate those optical quadruple systems that suffer only from the central concentration degeneracy.

Optical double systems suffer from both the central concentration degeneracy and the paucity of constraints. As they have no internal redundancy, their usefulness will depend upon the scatter in H_0 values observed from a good-sized sample of such systems.

In the case of B1608+656, the outstanding question is whether the data are so good that, merging lenses notwithstanding, all plausible models give the same value of H_0. What is needed now is the effort of a "loyal opposition" to search the far corners of model space.

New telescopes and upgrades to existing telescopes are certain to produce new gravitational lenses, and with them we will eventually see a Hubble constant that is less uncertain than that obtained from Cepheids. Even those who take it as a matter of faith that the universe is perfectly flat may find such a direct measurement of H_0 interesting.

Acknowledgements

References

Abazajian, K., et al. 2004, AJ, 128, 502

Barkana, R., Lehár, J., Falco, E. E., Grogin, N. A., Keeton, C. R., & Shapiro, I. I. 1999, ApJ, 520, 479

Bennett, C. L., *et al.* 2003, ApJS, 148, 1

Biggs, A. D., Browne, I. W. A., Helbig, P., Koopmans, L. V. E., Wilkinson, P. N., & Perley, R. A. 1999, MNRAS, 304, 349

Biggs, A. D., Wucknitz, O., Porcas, R. W., Browne, I. W. A., Jackson, N. J., Mao, S., & Wilkinson, P. N. 2003, MNRAS, 338, 599

Browne, I. W. A., Patnaik, A. R., Walsh, D., & Wilkinson, P. N. 1993, MNRAS, 263, L32

Burud, I., *et al.* 2000, ApJ, 544, 117

Chen, G. H., Kochanek, C. S., & Hewitt, J. N. 1995, ApJ, 447, 62

Cohn, J. D., Kochanek, C. S., McLeod, B. A., & Keeton, C. R. 2001, ApJ, 554, 1216

Courbin, F. 2003 Gravitational Lensing: a unique tool for cosmology, 000. (preprint: astro-ph/0304497)

Cristiani, S., Trentini, S., La Franca, F., Aretxaga, I., Andreani, P., Vio, R., & Gemmo, A. 1996, AAp, 306, 395

Fassnacht, C. D., Xanthopoulos, E., Koopmans, L. V. E., & Rusin, D. 2002, ApJ, 581, 823

Freedman, W. L., et al. 2001, ApJ, 553, 47

Gorenstein, M. V., Shapiro, I. I., & Falco, E. E. 1988, ApJ, 327, 693

Kochanek, C. S. 1995, ApJ, 445, 559

Kochanek, C. S., et al. 2000, ApJ, 543, 131

Kochanek, C. S. 2002, ApJ, 578, 25

Kochanek, C. S. & Schechter, P. L. 2004, Measuring and Modeling the Universe, 117

Koopmans, L. V. E., Treu, T., Fassnacht, C. D., Blandford, R. D., & Surpi, G. 2003, ApJ, 599, 70

Narayan, R. & Bartelmann, M. 1999, Formation of Structure in the Universe, 360

Ofek, E. O. & Maoz, D. 2003, ApJ, 594, 101

Patnaik, A. R., Browne, I. W. A., King, L. J., Muxlow, T. W. B., Walsh, D., & Wilkinson, P. N. 1992, Lecture Notes in Physics, Berlin Springer Verlag, 406, 140

Press, W. H. 1996, IAU Symp. 173: Astrophysical Applications of Gravitational Lensing, 173, 407

Refsdal, S. 1964, MNRAS, 128, 307

Romanowsky, A. J. & Kochanek, C. S. 1999, ApJ, 516, 18

Saha, P. 2000, AJ, 120, 1654

Schechter, P. L., et al. 1997, ApJL, 475, L85

Schechter, P. L. 2009, IAU Symposium, 201, 000 (preprint: astro-ph/0009048)

Schechter, P. L., et al. 2003, ApJ, 584, 657

Tegmark, M., *et al.* 2004, ApJ, 606, 702

Tegmark, M., *et al.* 2004, PRD, 69, 3501

Tonry, J. L. 1998, AJ, 115, 1

Tonry, J. L., *et al.* 2003, ApJ, 594, 1

Treu, T. & Koopmans, L. V. E. 2002, MNRAS, 337, L6

Udalski, A., Kubiak, M., & Szymański, M. 1997, Acta Astronomica, 47, 319

Vanden Berk, D. E., *et al.* 2004, ApJ, 601, 692

Williams, L. L. R. & Saha, P. 2000, AJ, 119, 439

Williams, L. L. R. & Schechter, P. L. 1997, Astronomy and Geophysics, 38, 10

Winn, J. N., Rusin, D., & Kochanek, C. S. 2004, Nature, 427, 613

Wyrzykowski, L., et al. 2003, Acta Astronomica, 53, 229

Wucknitz, O., Biggs, A. D., & Browne, I. W. A. 2004, MNRAS, 349, 14

York, T., Jackson, N., Browne, I. W. A., Wucknitz, O., & Skelton, J. E. 2004, preprint (astro-ph/0405115)